Two inherent crossovers of the diffusion process in glass-forming liquids

Maiko Kofu,[1,*] Antonio Faraone,[2,3] Madhusudan Tyagi,[2,3] Michihiro Nagao,[2,4] and Osamu Yamamuro[1,†]

[1]*Institute for Solid State Physics, University of Tokyo, Kashiwa, Chiba 277-8581, Japan*

[2]*NIST Center for Neutron Research, National Institute of Standards and Technology, Gaithersburg, Maryland 20899-6102, USA*

[3]*Department of Materials Science, University of Maryland, College Park, Maryland 20742, USA*

[4]*Center for Exploration of Energy and Matter, Indiana University, Bloomington, Indiana 47408-1398, USA*

(Received 15 April 2018; published 5 October 2018)

We report on incoherent quasielastic neutron scattering measurements examining a self-diffusion process in two types of glass-forming liquids, namely a molecular liquid (3-methylpentane) and an ionic liquid [1-butyl-3-methylimidazolium bis(trifluoromethanesulfonyl)imide]. We have experimentally demonstrated that both liquids exhibit two crossovers in the momentum transfer (Q) dependence of the self-correlation function, which is basically described by the stretched exponential function, $\exp[-(t/\tau)^{\beta}]$. The first crossover point ($Q \approx 0.2$ Å^{-1}) corresponds to a crossover from Fickian ($\beta = 1$) to non-Fickian ($\beta \neq 1$) diffusion attributed to dynamical correlation. On the other hand, the second one at $Q \approx 0.8$ Å^{-1} is associated with the crossover from Gaussian to non-Gaussian behavior. It is remarkable that the stretching exponent β gradually changes in between the two crossover points. We consider that the two crossovers are the universal feature for glass-forming liquids.

DOI: 10.1103/PhysRevE.98.042601

I. INTRODUCTION

It has been believed that the self-diffusion of molecules in a liquid is basically governed by Fick's law. The self-part of the van Hove correlation function $G_s(r, t)$ is written as a Gaussian function with respect to r and decays exponentially with t (Debye relaxation). Incoherent quasielastic neutron scattering (IQENS) experimentally gives the Fourier transform of $G_s(r, t)$, the incoherent dynamical structure factor $S_i(Q, \omega)$, or the incoherent intermediate scattering function $I_s(Q, t)$, where Q and ω are the momentum and energy transfer. In the case of Fickian diffusion, the relaxation obeys the relation $I_s(Q, t) = \exp(-t/\tau) = \exp(-DQ^2t)$, where D denotes the self-diffusion coefficient and τ is the relaxation time. On the other hand, the diffusion process in supercooled liquids is typically characterized by the non-Debye KWW (Kohlrausch-Williams-Watts) function, $\exp[-(t/\tau)^{\beta}]$, where the exponent β is a stretching parameter accounting for the deviations from the simple exponential behavior. A natural question arises as to whether the relation $\tau \propto Q^{-2}$ is valid for the non-Debye diffusion process. Many attempts to understand the nature of dynamics in the supercooled regime, including its Q-dependence, have been made by theoretical calculations/simulations [1–19] and quasielastic neutron scattering experiments [20–33].

A crossover in the Q-dependence of self-correlation functions was first discussed in glass-forming polymers [11,14,20–30]. Both IQENS and molecular-dynamics (MD) simulations have shown that the relaxation time follows the relation $\tau(Q) \propto Q^{-2/\beta}$ below Q_2 while $\tau(Q) \propto Q^{-2}$ above Q_2, where Q_2 roughly corresponds to the first maximum of the static structure factor $S(Q)$. The change at Q_2 is interpreted as a crossover from Gaussian at lower Q to non-Gaussian nature at higher Q. Additional crossover, which occurs at Q_1 ($< Q_2$), is reported for supercooled glycerol [31,33] and monomer species of polymer [17]. The relaxation time is proportional to Q^{-2} below Q_1, which is expected for the ordinary Fickian diffusion. Note that the absence of the crossover at Q_1 in polymers is a consequence of the chain connectivity of macromolecules giving rise to a different type of dynamics, namely Rouse dynamics.

The two crossovers have so far been found by MD simulations and fragmentally observed in IQENS experiments [17,31,33]. Only in glycerol is the detailed Q-dependence of τ and β investigated experimentally [31]. However, $I_s(Q, t)$ are plotted against reduced times estimated assuming the scaling of the characteristic time τ, viscosity η, and temperature [$\tau \propto \eta(T)/T$]; the data taken at different temperatures are combined to make a single master $I_s(Q, t)$ curve covering the whole Q region. Therefore, there remains serious ambiguity in the spatial scale dependence of diffusion behavior, especially in the variation of β.

In this paper, we demonstrate that $I_s(Q, t)$ exhibits the two crossovers in two different types of liquids, namely a molecular liquid (3-methylpentane) and an ionic liquid [1-butyl-3-methylimidazolium bis(trifluoromethanesulfonyl)imide, C4mimTFSI], using *real* experimental data. Molecular structures of both liquids are shown in Fig. 1. The glass transition temperatures (T_g) are reported to be 77 K for 3MP [34] and 181.5 K for C4mimTFSI [35]. There are several types of glasses, including network glass, molten salt glass, molecular glass, hydrogen-bond glass, metallic glass, and polymer glass. Glycerol is an example of hydrogen bond

*Present address: J-PARC Center, Japan Atomic Energy Agency, Tokai, Ibaraki 319-1195, Japan; maiko.kofu@j-parc.jp

†yamamuro@issp.u-tokyo.ac.jp

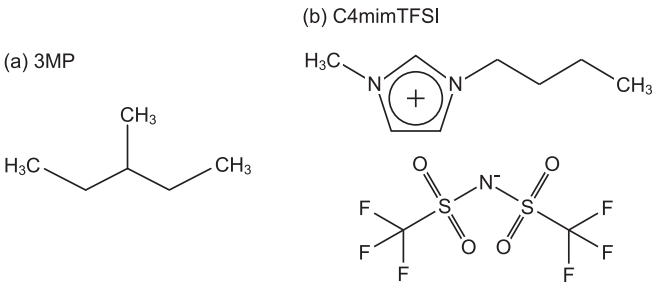

FIG. 1. Molecular (ionic) structures of (a) 3-methylpentane (3MP) and (b) 1-butyl-3-methylimidazolium bis(trifluoromethanesulfonyl)imide (C4mimTFSI).

glass and 3MP is a typical molecular glass. Ionic liquids are intermediate between molecular and molten salt glasses due to their amphipathic nature. The study on 3MP and C4mimTFSI, including the previous results on glycerol, allows us to clarify whether the crossover is a generic feature in the diffusion process of glass-forming liquids.

II. EXPERIMENT

3MP and C4mimTFSI, whose purities were better than 99.9%, were purchased from Tokyo Chemical Industry Co., Ltd. and Kanto Chemical Co., Inc., respectively, and used without further purification. IQENS experiments were performed on a neutron spin echo spectrometer (NSE) [36,37], a high-flux backscattering spectrometer (HFBS) [38], and a disk chopper time-of-flight spectrometer (DCS) [39] at the NIST Center for Neutron Research (NCNR) of the National Institute of Standards and Technology (NIST) in the United States. For 3MP and C4mimTFSI, the observed scattering signal is dominated by the incoherent scattering from H atoms, and so we measure the time evolution of self-diffusion of tagged particles (H atoms).

The measurements on NSE were performed using neutron wavelengths (λ) of 4.5, 6, and 8 Å with a distribution of $\Delta\lambda/\lambda = 0.15$ at a total Q range from 0.15 to 1.0 Å^{-1}. The range of Fourier times was between 4 ps and 35 ns. The HFBS instrument was operated in both fixed window and dynamic window modes. In the dynamic window mode for IQENS experiments, Doppler-shifted neutrons with $\lambda = 6.27$ Å allow the investigation of the dynamic range of ± 15 μeV with an energy resolution of 0.8 μeV (full width at half-maximum). The Q-range covered by HFBS was $0.25 \leqslant Q \leqslant 1.75$ Å^{-1}. As for C4mimTFSI having fast local motions, the IQENS measurement was also done on DCS utilizing incident neutrons of 6 and 9 Å with corresponding resolutions of 64 and 22 μeV and maximum Q's of 1.3 and 1.9 Å^{-1}. The use of these three spectrometers enabled us to investigate the diffusion dynamics in wide time (1 ps to 100 ns) and Q (0.15–1.7 Å^{-1}) ranges. The data were corrected at 127 K for 3MP and at 300 K for C4mimTFSI, which correspond to $1.65T_g$. The temperatures were chosen to examine the Q-dependence of diffusion dynamics in the accessible time range by the neutron spectrometers used. The data were also recorded below 10 K to obtain the instrumental resolutions.

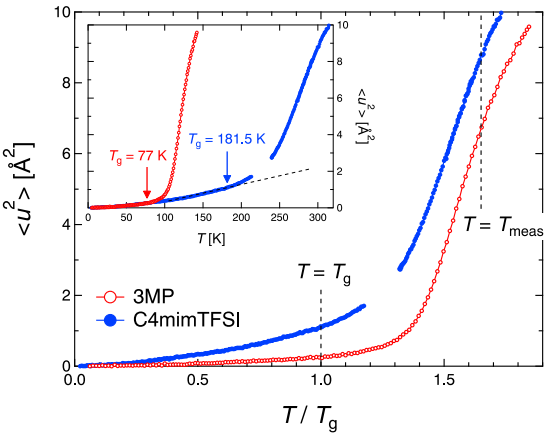

FIG. 2. Mean-square displacements $\langle u^2 \rangle$ of 3MP and C4mimTFSI as a function of T/T_g taken on HFBS. Temperatures of glass transitions (T_g) and IQENS measurements (T_{meas}) are denoted. The inset shows the temperature dependence of $\langle u^2 \rangle$ and the dashed line displays an expectation for a harmonic oscillator.

The data reduction and Fourier transform of $S_i(Q, \omega)$ data were performed using the DAVE software package [40], and we discuss only $I_s(Q, t)$ in this paper.

III. RESULTS AND DISCUSSION

Elastic fixed window scans were performed first on the HFBS instrument to obtain the mean-square displacement $\langle u^2 \rangle$ in a wide temperature range. $\langle u^2 \rangle$ is evaluated from the equation $S(Q, \omega) \propto \exp(-\langle u^2 \rangle Q^2/3)$. The temperature dependence of $\langle u^2 \rangle$ for both liquids is presented in Fig. 2. This plot is helpful to see at what temperatures the dynamics enters the time window of the neutron spectrometer. The $\langle u^2 \rangle$ data between 213 and 240 K for C4mimTFSI are missing due to crystallization. At around T_g, $\langle u^2 \rangle$ displays a clear upturn, indicating that some relaxation gets activated. It should be emphasized that $\langle u^2 \rangle$ of 3MP steeply increases above $T \simeq 1.3T_g$ while that of C4mimTFSI gradually increases. The results are indicative of multiple relaxation processes in C4mimTFSI and a single process in 3MP.

Figure 3 shows the normalized intermediate scattering functions, $I_s(Q, t)/I_s(Q, 0)$, at several Q's between 0.15 and 1.0 Å^{-1}. The data measured on two or three spectrometers are combined to produce the real $I_s(Q, t)$ curves in the time range of four orders of magnitude. Note that scale factors are applied to match the values among different spectrometers with different energy windows. This procedure is often required because $I_s(Q, 0)$ is practically obtained by the integration over the finite energy region that is specific to the spectrometers. No scale factor was applied for the data of NSE and DCS with $\lambda = 6$ Å, where the integral range is about ± 1 meV, while the scale factors larger than 1 were multiplied for the other data with narrower integral ranges. In both liquids, clear relaxation processes were observed. The self-correlation function decays faster at higher Q, which is characteristic of the diffusion process. Apparently, the shape of the self-correlation function varies depending on Q; the higher Q is, the more gradually it decays in a wider time range.

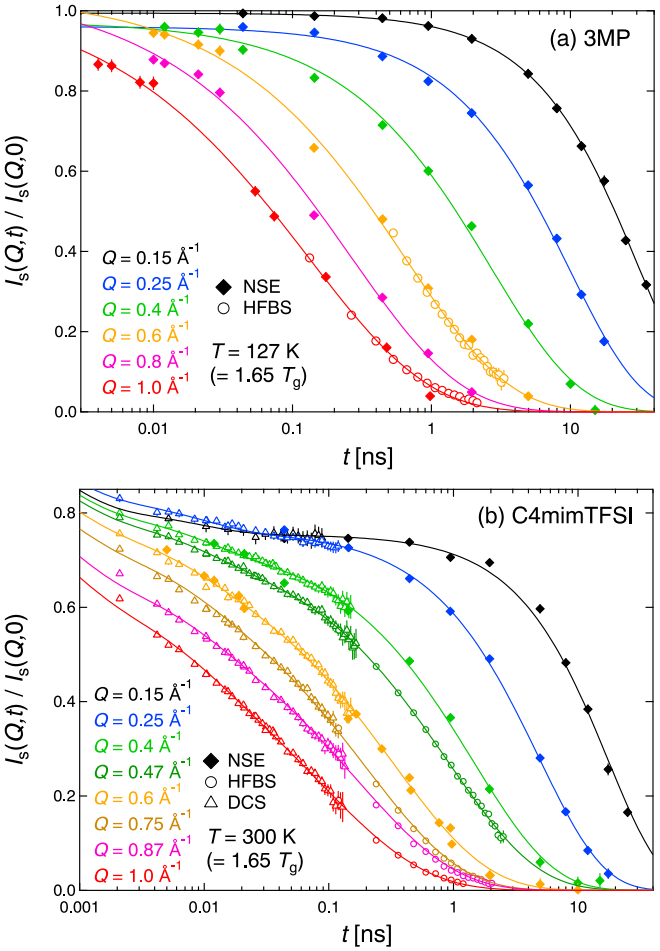

FIG. 3. Normalized intermediate scattering functions of (a) 3MP at 127 K and (b) C4mimTFSI at 300 K for several Q values from 0.15 to 1.0 Å^{-1}.

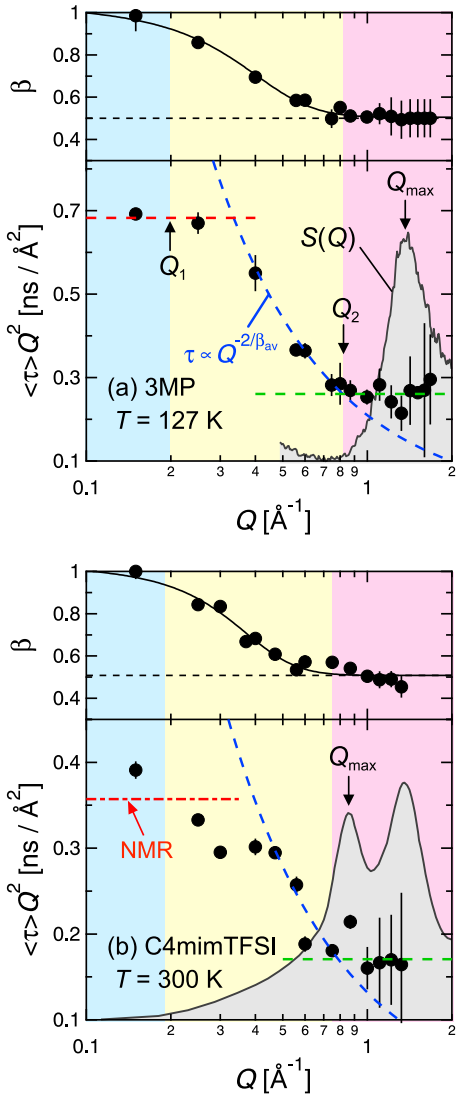

FIG. 4. Mean relaxation times multiplied by Q^2 and the exponents β of KWW functions against Q for (a) 3MP at 127 K and (b) C4mimTFSI at 300 K. Static structure factors $S(Q)$ are also shown as gray shaded areas. In the upper panels, horizontal dashed lines show $\beta = 0.5$ and solid curves are guides for the eyes. In the lower panels, dashed red and green lines represent the $\tau \propto Q^2$ behavior and dashed blue curves denote $\tau \propto Q^{2/\beta_{av}}$ ($\beta_{av} = 0.65$). The dash-dotted red line corresponds to D^{-1} estimated from the PFG-NMR experiment [42]. Q_1 and Q_2 are the Q positions at which crossover occurs and Q_{max} at the first maximum in $S(Q)$.

The self-correlation functions of 3MP were well fitted to a single KWW function,

$$\frac{I(Q,t)}{I(Q,0)} = Ae^{-(\frac{t}{\tau_{KWW}})^{\beta}}. \quad (1)$$

The obtained prefactor A was roughly 1, indicating that damping of vibration and any other local relaxation hardly occur at a temperature as low as 127 K. One may consider that rotations of CH_3 group could be observed even at low temperatures. However, in the present data of 3MP, the CH_3 rotations were not independently observed from the translation diffusion. The absence of CH_3 rotations is also supported by the temperature dependence of $\langle u^2 \rangle$ (Fig. 2); there is no sign of the relaxation process below $1.3T_g$. Perhaps inter- and intramolecular interactions in 3MP can cause high potential barriers for the rotations. On the other hand, local relaxation processes were clearly observed in C4mimTFSI. The relaxation curves of C4mimTFSI were fitted with the combination of exponential and KWW functions,

$$\frac{I(Q,t)}{I(Q,0)} = A_0e^{-\frac{t}{\tau_0}} + A_1e^{-\frac{t}{\tau_1}} + A_2e^{-(\frac{t}{\tau_{KWW}})^{\beta}}. \quad (2)$$

The two exponential terms are attributed to fast local processes, and their relaxation times were fixed to the literature values ($\tau_0 = 0.66$ ps, $\tau_1 = 8.97$ ps) [41]. A_i is the fraction of each relaxation, and a constraint, $A_0 + A_1 + A_2 = \exp(-2W)$, was applied. Here, $\exp(-2W)$ is known as the Debye-Waller factor and was estimated from the elastic scattering signals taken on DCS.

The product of the mean relaxation time and Q^2, $\langle \tau \rangle Q^2$, and β are plotted against Q in Fig. 4. The mean relaxation time is evaluated using the relation $\langle \tau \rangle = \tau_{KWW}/\beta\Gamma(1/\beta)$ (Γ is the Gamma function). Note that $\langle \tau \rangle Q^2$ is constant ($= 1/D$) when the Fickian diffusion dynamics is observed. It is

evident that the character of tagged particle motion changes at $Q = Q_1$ ($\approx$0.2 Å^{-1}) and Q_2 ($\approx$0.8 Å^{-1}) in both liquids. Interestingly, β also changes at these Q's. Below Q_1, $\langle\tau\rangle Q^2$ is almost constant (red lines in Fig. 4) and β is approximately 1. Although the data of C4mimTFSI fluctuate due to the presence of the fast local relaxation processes, the data are in rough agreement with the value of D^{-1} obtained from a pulsed field gradient nuclear magnetic resonance (PFG-NMR) experiment ($Q < 2 \times 10^{-4}$ Å^{-1}) [42] (dash-dotted red line). Therefore, it appears reasonable to conclude that the process below Q_1 is the Fickian diffusion. In the intermediate region ($Q_1 < Q < Q_2$), the Q-dependence of $\langle\tau\rangle$ is steeper than Q^{-2}. $I_s(Q,t)$ is not reproduced by the exponential function but by the KWW one. The exponent β decreases with increasing Q and reaches 0.5 at Q_2. Above Q_2, the relaxation times again follow the relation $\tau \propto Q^{-2}$ (dashed green line), but β remains almost constant at 0.5. The variations of τ and β with Q are qualitatively similar among 3MP, C4mimTFSI, and glycerol [31], though the glycerol data have ambiguity caused by the reduced time. These results suggest that the appearance of the two crossovers is generic behavior in supercooled liquids.

Dashed blue curves in Fig. 4 show the relation $\tau \propto Q^{-2/\beta_{av}}$ implying the Gaussian nature, which is reported in previous works [11,14,17,20–31,33]. Here the average values of the stretching parameter, $\beta_{av} = 0.65$, were used. The relation holds in a narrow Q region $0.4 < Q < 0.8$ Å^{-1} for 3MP and C4mimTFSI at $T = 1.65T_g$. This could be due to the relative proximity of Q_1 to Q_2. We anticipate that as the system is further cooled, the first crossover occurs at a lower Q and the $\tau \propto Q^{-2/\beta}$ relation is confirmed in a wider Q region.

Figure 4 also presents the static structure factor $S(Q)$ of fully deuterated 3MP obtained at 140 K with a neutron scattering spectrometer SWAN at KENS, High Energy Accelerator Research Organization, Japan, and the $S(Q)$ of C4mimTFSI at room temperature with an x-ray diffraction instrument [43]. The first maximum in $S(Q)$, Q_{max}, is situated at 1.4 Å^{-1} for 3MP and 0.85 Å^{-1} [44] for C4mimTFSI. The crossover occurs at a similar Q_2 ($\approx$0.8 Å^{-1}) in both liquids, but Q_{max} is somewhat different. The length scale of Q_2 is about 8 Å and roughly corresponds to the average intermolecular distance. In regard to the position of Q_2, our result is consistent with those reported previously; the crossover point Q_2 is located in the range of 0.6–1.0 Å^{-1} and close to but slightly lower than Q_{max} in polymers [11,14,20–30] and glycerol [31,33].

We now discuss microscopic molecular motions detected in the time and spatial scales of neutron scattering. In glass-forming liquids, even at temperatures well above T_g ($T = 1.65T_g$ in the present case), molecules correlate with each other and they move cooperatively. The dynamically correlated region is rather small and its size is about the intermolecular distance in the temperature range. The structural correlation causes the sluggish cooperative motion, where memory effects play an essential role in the dynamics. Such a motion is characterized by the KWW function.

In IQENS experiments, τ at a given Q corresponds to an average time for a tagged particle stepping out of the region with a size of $2\pi/Q$ (see Fig. 5). Therefore, both

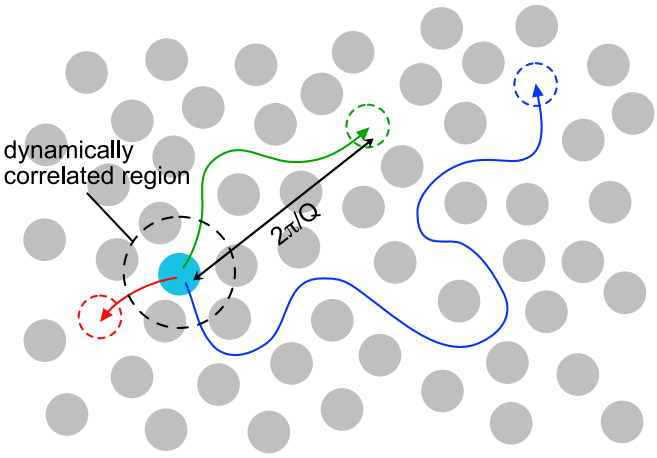

FIG. 5. Schematic illustration of the diffusion process in short (red, $Q > Q_2$), medium (green, $Q_1 < Q < Q_2$), and long (blue, $Q < Q_1$) spatial scales.

crossovers could be discussed in terms of "spatial averaging." In the Q region above Q_2, the corresponding spatial region is rather small, and the tagged particle experiences only one or two jumps to leave the region (red process in Fig. 5). In that case, the particles still remember where they were in the recent past due to the short-range correlations. The motions of tagged particles inside the correlated region would be rather heterogeneous, being associated with non-Gaussian behavior. When we take an average of the motions over the space larger than the correlated region ($Q_1 < Q < Q_2$; green process), all of the particles relax identically (Gaussian nature) but intrinsically exhibit KWW behavior due to the memory effect. In this transient region, the particle undergoes a sequence of jumps including backscattering events, which is often called subdiffusion, giving rise to the $\tau \propto Q^{-n}$ ($n > 2$) behavior. As Q is further decreased (the spatial region is increased), the memory effect fades away, which causes the increase in β toward 1. Below Q_1 with a length scale larger than 30 Å (blue process), the particle dynamics is highly coarse-grained in time and resembles the ordinary Fickian diffusion. It should be noted here that the memory effect is convoluted in the diffusion dynamics, even if the dynamics seems "uncorrelated." The effective diffusion coefficient with the memory effect could be smaller than that of the simple Fickian diffusion.

The previous MD simulation works have shown that the non-Gaussian parameter (NGP) exhibits a significant value above Q_2 [11,17,25–27,30,33]. Although the NGP is not estimated from our experiments, it is reasonable to consider that the Gaussianity changes at around Q_2. Colmenero, Arbe, and co-workers suggested that the crossover could also be understood as a homogeneous to heterogeneous crossover [11,22,23,25,26]. They proposed an anomalous jump diffusion model, where the heterogeneity is attributed to the distribution of the jump length. In this interpretation, the heterogeneity is inherent in polymers or liquids and not the same as the dynamical heterogeneity, which appears near T_g. In fact, the crossover at Q_2 remains almost unchanged in a wide temperature range ($1.5T_g < T < 2.5T_g$) [26]. This

picture is consistent with our interpretation of Q_2 described above.

Furthermore, some theoretical studies on supercooled liquids have shown that the mean-square displacement $\langle r^2 \rangle$ exhibits a complicated behavior in time; $\langle r^2 \rangle \propto t^2$ at very short times (ballistic motion), $\langle r^2 \rangle \propto t^\alpha$ ($\alpha < 1$) at intermediate times (subdiffusion), and $\langle r^2 \rangle \propto t$ at long times (diffusion). Upon cooling, such a complicated behavior is pronounced and NGP displays nonzero values in the intermediate (subdiffusive) region [2–4,6,8,9,11–13,16,17,25,26,30,33]. In the framework of mode-coupling theory (MCT) [45], the complex behavior in $\langle r^2 \rangle$ is referred to as a crossover from a localized cage motion to diffusion. The results of our experiment and previous works are qualitatively compatible with the MCT picture.

Finally, we comment on the change in β at Q_2 (see Fig. 4). The MD simulation works on liquids show that β increases toward 1 when Q is lowered as in our experiments, in contrast to polymers in which β remains almost unchanged. However, their Q-dependency is equivocal. β changes below $Q \approx 0.5$ Å^{-1} in glycerol [33], below $Q \approx 0.8$ Å^{-1} in monomer species of polymer [17], and gradually changes in a wide Q regime ($Q \leqslant 2$ Å^{-1}) in water [4] and orthoterphenyl [9], while most of the experimental data do not display a significant variation of β. It is often difficult to determine β in a wide Q-region due to the limitation of the time window in experiments. The relation between the nonexponentiality and the Gaussianity remains an open question, and further studies are required.

IV. SUMMARY

We have studied in detail the momentum transfer Q dependence of the self-diffusion process in two types of glass-forming liquids by means of IQENS. Several spectrometers with different time windows were used to obtain self-correlation functions in a wide time range. It was demonstrated that the diffusion behavior of molecules changes at two crossover points. Below the first crossover point ($Q_1 \approx 0.2$ Å^{-1}), the movement of the molecules asymptotically obeys Fick's raw ($\tau \propto Q^{-2}$). When Q is higher than Q_1, the intermediate scattering functions are well approximated by the KWW function. In addition, the exponent β gradually decreases with increasing Q and reaches 0.5 at the second crossover point ($Q_1 \approx 0.8$ Å^{-1}). In this transient region, the relation $\tau \propto Q^{-2}$ violates and another relation $\tau \propto Q^{-2/\beta}$ is observed in a narrow Q region. Above $Q = Q_2$, τ is again proportional to Q^{-2}, and β remains almost constant at 0.5.

Q_1 corresponds to the onset of non-Fickian diffusion attributed to dynamical correlation in supercooled liquids, while Q_2 is the crossover point from the Gaussian to the non-Gaussian character. The present results clearly provide the experimental evidence for the two crossovers and the Q dependence of β. They are qualitatively consistent with previous MD simulations and IQENS works. We conclude that the two crossovers are a generic feature in glass-forming liquids at relatively higher temperatures than T_g.

ACKNOWLEDGMENTS

We thank Toshiya Otomo (KENS) for his assistance in the SWAN experiment. Travel expenses for the experiments at NCNR were supported by General User Program for Neutron Scattering Experiments, Institute for Solid State Physics, The University of Tokyo (Proposal No. 15587), at JRR-3, Japan Atomic Energy Agency, Tokai, Japan. This work utilized facilities supported in part by the National Science Foundation under Agreement No. DMR-1508249. M.N. acknowledges funding support from the cooperative agreement 70NANB15H259 from NIST, U.S. Department of Commerce. Certain commercial equipment, instruments, or materials are identified in this paper to foster understanding. Such identification does not imply recommendation or endorsement by the National Institute of Standards and Technology, nor does it imply that the materials or equipment identified are necessarily the best available for the purpose.

[1] M. Fuchs, I. Hofacker, and A. Latz, Phys. Rev. A **45**, 898 (1992).
[2] W. Kob and H. C. Andersen, Phys. Rev. E **51**, 4626 (1995).
[3] M. M. Hurley and P. Harrowell, J. Chem. Phys. **105**, 10521 (1996).
[4] F. Sciortino, P. Gallo, P. Tartaglia, and S.-H. Chen, Phys. Rev. E **54**, 6331 (1996).
[5] F. Sciortino, L. Fabbian, S.-H. Chen, and P. Tartaglia, Phys. Rev. E **56**, 5397 (1997).
[6] M. Fuchs, W. Götze, and M. R. Mayr, Phys. Rev. E **58**, 3384 (1998).
[7] C. Bennemann, J. Baschnagel, and W. Paul, Eur. Phys. J. B **10**, 323 (1999).
[8] B. Doliwa and A. Heuer, J. Phys.: Condens. Matter **11**, A277 (1999).
[9] S. Mossa, R. Di Leonardo, G. Ruocco, and M. Sampoli, Phys. Rev. E **62**, 612 (2000).
[10] S.-H. Chong, W. Götze, and M. R. Mayr, Phys. Rev. E **64**, 011503 (2001).
[11] J. Colmenero, F. Alvarez, and A. Arbe, Phys. Rev. E **65**, 041804 (2002).
[12] R. Zangi and S. A. Rice, Phys. Rev. Lett. **92**, 035502 (2004).
[13] M. Kluge and H. R. Schober, Phys. Rev. B **70**, 224209 (2004).
[14] A. Neelakantan and J. K. Maranas, J. Chem. Phys. **120**, 465 (2004).
[15] L. Berthier, D. Chandler, and J. P. Garrahan, Europhys. Lett. **69**, 320 (2005).
[16] B. Vorselaars, A. V. Lyulin, K. Karatasos, and M. A. J. Michels, Phys. Rev. E **75**, 011504 (2007).
[17] J. Sacristan, F. Alvarez, and J. Colmenero, Europhys. Lett. **80**, 38001 (2007).
[18] J. Habasaki and K. L. Ngai, J. Chem. Phys. **133**, 124505 (2010).
[19] S. P. Niblett, V. K. de Souza, J. D. Stevenson, and D. J. Wales, J. Chem. Phys. **145**, 024505 (2016).
[20] J. Colmenero, A. Alegría, A. Arbe, and B. Frick, Phys. Rev. Lett. **69**, 478 (1992).
[21] D. Richter, A. Arbe, J. Colmenero, M. Monkenbusch, B. Farago, and R. Faust, Macromolecules **31**, 1133 (1998).

[22] A. Arbe, J. Colmenero, M. Monkenbusch, and D. Richter, Phys. Rev. Lett. **81**, 590 (1998).
[23] J. Colmenero, A. Arbe, A. Alegría, M. Monkenbusch, and D. Richter, J. Phys.: Condens. Matter **11**, A363 (1999).
[24] B. Farago, A. Arbe, J. Colmenero, R. Faust, U. Buchenau, and D. Richter, Phys. Rev. E **65**, 051803 (2002).
[25] A. Arbe, J. Colmenero, F. Alvarez, M. Monkenbusch, D. Richter, B. Farago, and B. Frick, Phys. Rev. Lett. **89**, 245701 (2002).
[26] A. Arbe, J. Colmenero, F. Alvarez, M. Monkenbusch, D. Richter, B. Farago, and B. Frick, Phys. Rev. E **67**, 051802 (2003).
[27] A. Narros, F. Alvarez, A. Arbe, J. Colmenero, D. Richter, and B. Farago, J. Chem. Phys. **121**, 3282 (2004).
[28] A.-C. Genix, A. Arbe, F. Alvarez, J. Colmenero, B. Farago, A. Wischnewski, and D. Richter, Macromolecules **39**, 6260 (2006).
[29] M. Tyagi, A. Arbe, A. Alegría, J. Colmenero, and B. Frick, Macromolecules **40**, 4568 (2007).
[30] S. Capponi, A. Arbe, F. Alvarez, J. Colmenero, B. Frick, and J. P. Embs, J. Chem. Phys. **131**, 204901 (2009).
[31] J. Wuttke, I. Chang, O. G. Randl, F. Fujara, and W. Petry, Phys. Rev. E **54**, 5364 (1996).
[32] J. Wuttke, W. Petry, and S. Pouget, J. Chem. Phys. **105**, 5177 (1996).
[33] R. Busselez, R. Lefort, A. Ghoufi, B. Beuneu, B. Frick, F. Affouard, and D. Morineau, J. Phys. Condens. Matter **23**, 505102 (2011).
[34] S. Takahara, O. Yamamuro, and H. Suga, J. Non-Cryst. Solids **171**, 259 (1994).
[35] A. V. Blokhin, Y. U. Paulechka, A. A. Strechan, and G. J. Kabo, J. Phys. Chem. B **112**, 4357 (2008).
[36] N. Rosov, S. Rathgeber, and M. Monkenbusch, in *Scattering from Polymers: Characterization by X-rays, Neutrons, and Light*, edited by P. Cebe, B. S. Hsiao, and D. J. Lohse, ACS Symp. Series 739 (American Chemical Society, Washington D.C., 2000), pp. 103–116.
[37] M. Monkenbusch, R. Schätzler, and D. Richter, Nucl. Instrum. Methods Phys. Res. Sect. A **399**, 301 (1997).
[38] A. Meyer, R. M. Dimeo, P. M. Gehring, and D. A. Neumann, Rev. Sci. Instrum. **74**, 2759 (2003).
[39] J. R. D. Copley and J. C. Cook, Chem. Phys. **292**, 477 (2003).
[40] R. T. Azuah, L. R. Kneller, Y. Qiu, P. L. W. Tregenna-Piggott, C. M. Brown, J. R. D. Copley, and R. M. Dimeo, J. Res. Natl. Inst. Stan. Technol. **114**, 341 (2009).
[41] M. Kofu, M. Tyagi, Y. Inamura, K. Miyazaki, and O. Yamamuro, J. Chem. Phys. **143**, 234502 (2015).
[42] H. Tokuda, K. Hayamizu, K. Ishii, M. A. B. H. Susan, and M. Watanabe, J. Phys. Chem. B **108**, 16593 (2004).
[43] D. Xiao, L. G. Hines, Jr., S. Li, R. A. Bartsch, E. L. Quitevis, O. Russina, and A. Triolo, J. Phys. Chem. B **113**, 6426 (2009).
[44] It is known that a prepeak appears at $Q = 0.2$–0.4 Å^{-1} for imidazolium-based ionic liquids with longer alkyl-chains. The low-Q peak is associated with the nanoscale segregation between polar and nonpolar entities. The peak at $Q = 0.85$ Å^{-1} corresponds to the correlation between adjacent polar entities.
[45] W. Götze and L. Sjögren, Rep. Prog. Phys. **55**, 241 (1992).